Geophysical Research Letters

Supporting Information for

Mesoscale eddies enhance the air-sea CO_2 sink in the South Atlantic Ocean

Daniel J. Ford[1,2,*], Gavin H. Tilstone[1], Jamie D. Shutler[2], Vassilis Kitidis[1], Katy L. Sheen[2], Giorgio Dall'Olmo[1,†] and Iole B.M. Orselli[3]

[1] Plymouth Marine Laboratory, Plymouth, UK
[2] College of Life and Environmental Sciences, University of Exeter, Penryn, UK
[3] Laboratório de Estudos dos Oceanos e Clima, Instituto de Oceanografia, Universidade Federal do Rio Grande (FURG), Av. Itália km 8, s/n, Rio Grande, 96203-900 RS, Brazil

[*] now at: Faculty of Environment, Science and Economy, University of Exeter, Penryn, UK
[†] now at: Istituto Nazionale di Oceanografia e di Geofisica Sperimentale, Borgo Grotta Gigante 42/c, 34010 Sgonico, Trieste, Italy

Contents of this file

Supplementary Materials A to D

Supplementary A – Eddy tracking example

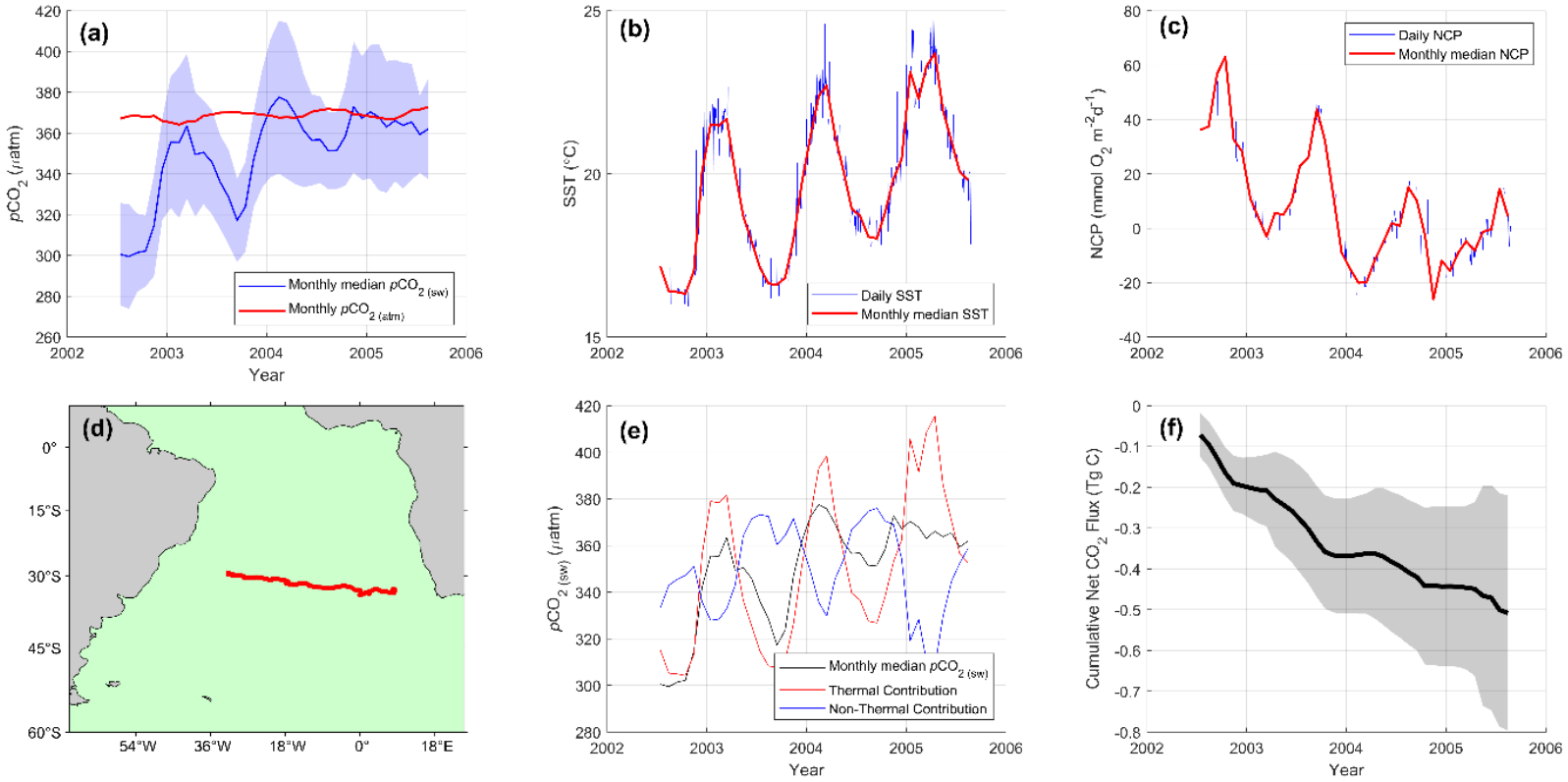

Figure. S1: Example output from the Lagrangian eddy tracking approach for an anticyclonic eddy. (a) Blue line indicates the monthly $pCO_{2\ (sw)}$ estimated with the SA-FNN$_{NCP}$, and shading indicates the uncertainty on the SA-FNN$_{NCP}$ retrieval. Red line indicates the monthly atmospheric pCO_2 for the mean location of the eddy in the respective month. (b) Blue line indicates the daily sea surface temperature (SST) for the eddy lifetime. Red line shows the calendar month medians of SST. (c) Blue line indicates the daily net community production (NCP) for the eddy lifetime. Red line shows the calendar month medians of NCP. (d) Red line shows the geographic track of the eddy over the lifetime. (e) Black line indicates the monthly $pCO_{2\ (sw)}$. Red line indicates the thermal contribution and blue line indicates the non-thermal contribution to the $pCO_{2\ (sw)}$ variability. (f) Black line shows the cumulative net CO_2 flux, where the shading indicates he 95% confidence interval.

Supplementary B – Comparison of SA-FNN$_{NCP}$ and in situ $pCO_{2\,(sw)}$ within mesoscale eddies

The global ocean ship-based hydrographic investigations program (GO-SHIP) research cruises conduct hydrographic observations which include Dissolved Inorganic Carbon (DIC) and Total Alkalinity (TA) along CLIVAR/WOCE repeat hydrographic sections. Transects within the South Atlantic Ocean between 2002 and 2018 were downloaded from the NODC/NOAA data centre (https://www.ncei.noaa.gov/access/ocean-carbon-data-system/oceans/RepeatSections/, last accessed: 29/09/2021), which included sections A10 (2003; 2011; 2017), A9.5 (2009; 2018), A13.5 (2013) and A16S (2005; 2013; Fig. S2 a). Each transect was analysed for measurements which coincided with anticyclonic or cyclonic eddies tracked in our study. $pCO_{2\,(sw)}$ was calculated from DIC and TA using CO2SYSv3 (van Heuven et al., 2011; Lewis et al., 1998; Orr et al., 2018; Sharp et al., 2021), and the reported uncertainties in DIC (~2 $\mu molkg^{-1}$), TA (~2 $\mu molkg^{-1}$), carbonic acid (Waters et al., 2014) and H_2SO_4 dissociation constants (Dickson, 1990) were propagated to retrieve the $pCO_{2\,(sw)}$ uncertainty. The *in situ* $pCO_{2\,(sw)}$ were corrected to a consistent temperature and depth dataset (Reynolds et al., 2002), following the methodology described in Goddijn-Murphy et al. (2015), to be consistent with the SA-FNN$_{NCP}$ sub skin $pCO_{2\,(sw)}$ observations (Ford et al., 2022; Woolf et al., 2016).

The Following Ocean Rings in the South Atlantic (FORSA) cruise, sampled six anticyclonic eddies with a continuous underway $pCO_{2\,(sw)}$ system, described in Orselli et al. (2019). These $pCO_{2\,(sw)}$ observations were reanalysed to a consistent temperature and depth dataset (Goddijn-Murphy et al., 2015; Reynolds et al., 2002) using the "fe_reanalyse_socat.py" functions within the open source FluxEngine (Holding et al., 2019; Shutler et al., 2016), and the cruise track analysed for anticyclonic and cyclonic eddies tracked in our study. The mean and standard deviation of in situ $pCO_{2\,(sw)}$ for matching eddies were extracted for the region within the AVISO+ eddy radius.

In total six anticyclonic (GO-SHIP = 4; FORSA = 2; Fig. S2a) and two cyclonic (GO-SHIP = 1; FORSA = 1; Fig. S2b) eddies tracked in our study were sampled *in situ.* The *in situ* $pCO_{2\,(sw)}$ were compared with the SA-FNN$_{NCP}$ $pCO_{2\,(sw)}$ estimates for the month the eddy was sampled *in situ* (Fig. S2c). The SA-FNN$_{NCP}$ $pCO_{2\,(sw)}$ estimates were accurate compared to the $pCO_{2\,(sw)}$ in anticyclonic eddies with a low root mean square difference (RMSD; 10.2 µatm; Fig. S2c) but showed a higher RMSD for the cyclonic eddies (20.9 µatm; Fig S2c), although this was lower than the SA-FNN$_{NCP}$ accuracy (21.48 µatm) (Ford et al., 2022).

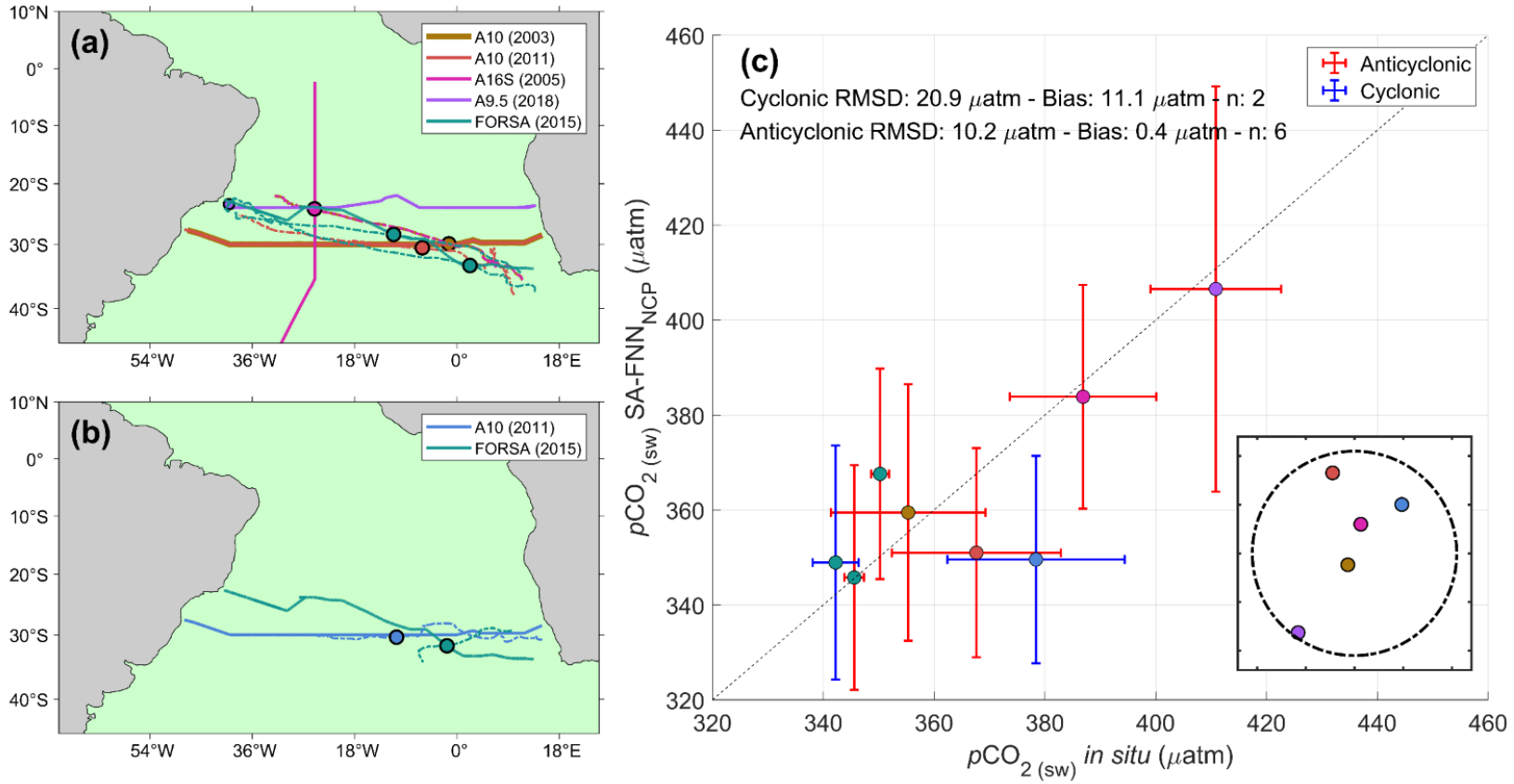

Figure. S2: (a) Dashed coloured lines indicate the trajectories of tracked anticyclonic eddies that were sampled *in situ*, where the sampling location is highlighted by the same coloured point. Solid coloured lines indicate cruise tracks which sampled the respective eddy. (b) Same as (a) but for cyclonic eddies. (c) Comparison of in situ $pCO_{2\,(sw)}$ with SA-FNN_{NCP} $pCO_{2\,(sw)}$ for anticyclonic (red errorbars) and cyclonic eddies (blue errorbars). Central coloured point represents the respective eddy sampled in (a) or (b). In plot statistics are root mean square deviation (RMSD), bias and the number of eddies (n). Inset indicates an eddy centric diagram identifying the location the *in situ* stations sampled (coloured points) with respect to the eddy radius (dashed line). Note the FORSA cruise sampled $pCO_{2\,(sw)}$ continuously and therefore does not appear on the inset.

Supplementary C – Are mesoscale eddies distinct from their environment?

Daily anomalies in MODIS-A SST, SSS and NCP within both anticyclonic and cyclonic eddies were calculated with respect to the environmental conditions surrounding the eddy (described in section 2.2). The daily anomalies were fit with a 'smoothing spline' function within MATLAB (smoothing parameter = 4.14×10^{-7}) to identify the longer term variations in the anomalies for each eddy (Fig. S3; Fig. S4). The anticyclonic eddies generally showed initial positive SST (Fig. S3a) and SSS (Fig. S3b) anomalies, which were converted to negative SST anomalies within ~6 months from the start of eddy tracking. The strength of negative SST anomalies were generally greater in austral winter, than summer. SSS anomalies indicated a linear decrease over time, as the eddy moved into the South Atlantic gyre. The cyclonic eddies showed initial negative SST anomalies which rapidly increase to ~ 0, but with seasonal fluctuations (Fig. S3c). The SSS anomalies however showed no clear pattern and were generally weak (Fig.S3d).

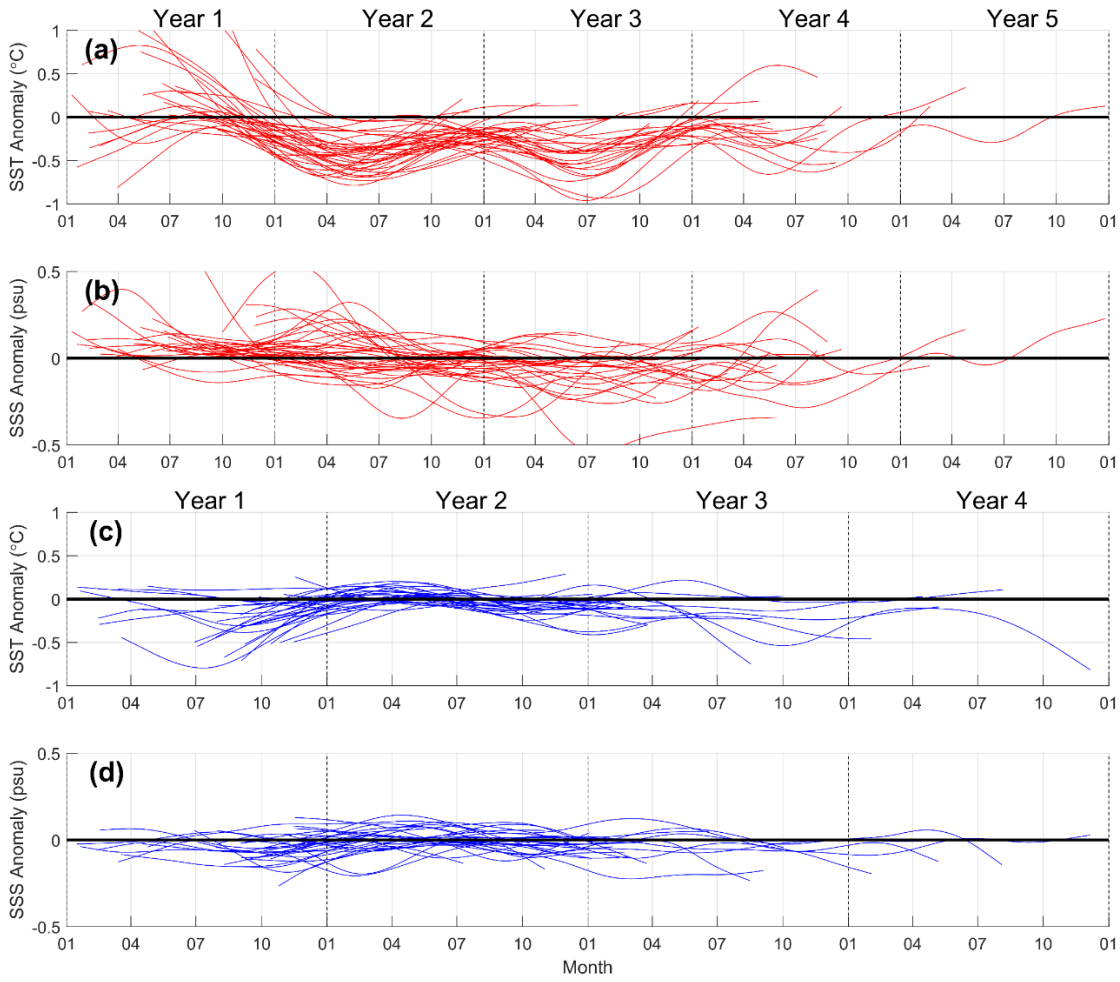

Figure S3: Smoothed anomalies in physical parameters (SST and SSS) within mesoscales eddies with respect to the environmental conditions. (a) and (c) show SST anomalies for anticyclonic (Agulhas) and cyclonic eddies respectively. (b) and (d) show SSS anomalies for anticyclonic (Agulhas) and cyclonic eddies respectively. Black solid line indicates an anomaly of 0.

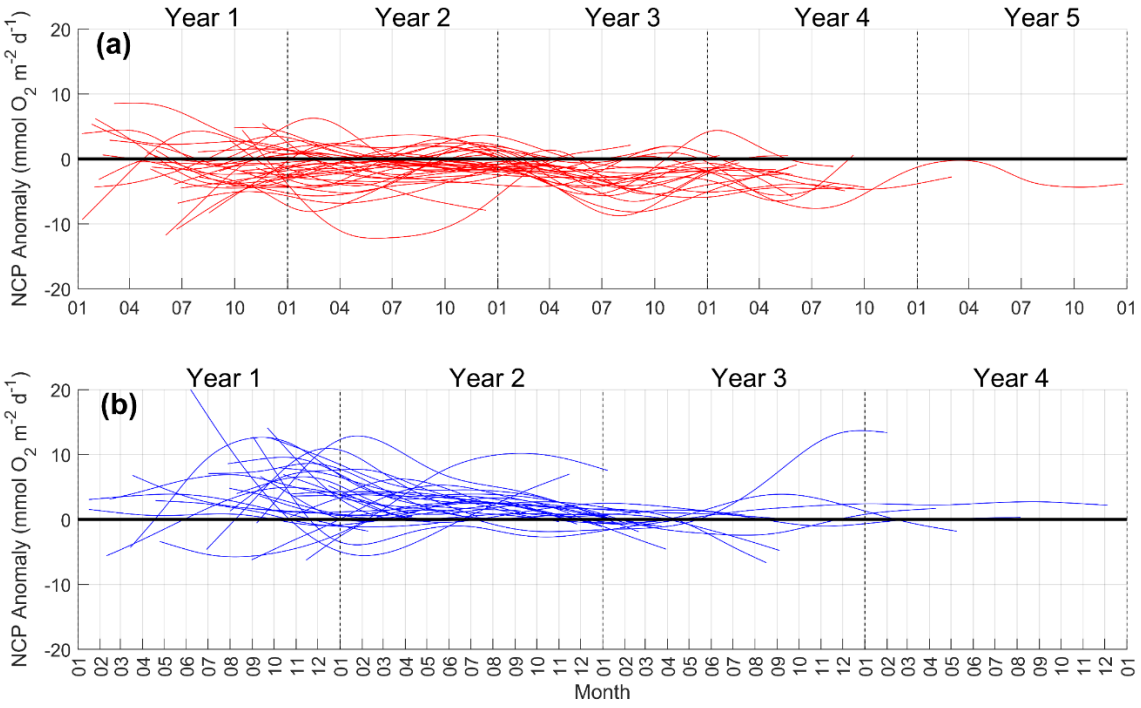

Figure S4: Smoothed anomalies in NCP within mesoscale eddies with respect to the environmental conditions. (a) shows the NCP anomalies for anticyclonic (Agulhas) eddies, and (b) the same for cyclonic eddies. Black line indicates an anomaly of 0.

Supplementary D – Comparison of using different eddy radii to determine environmental conditions

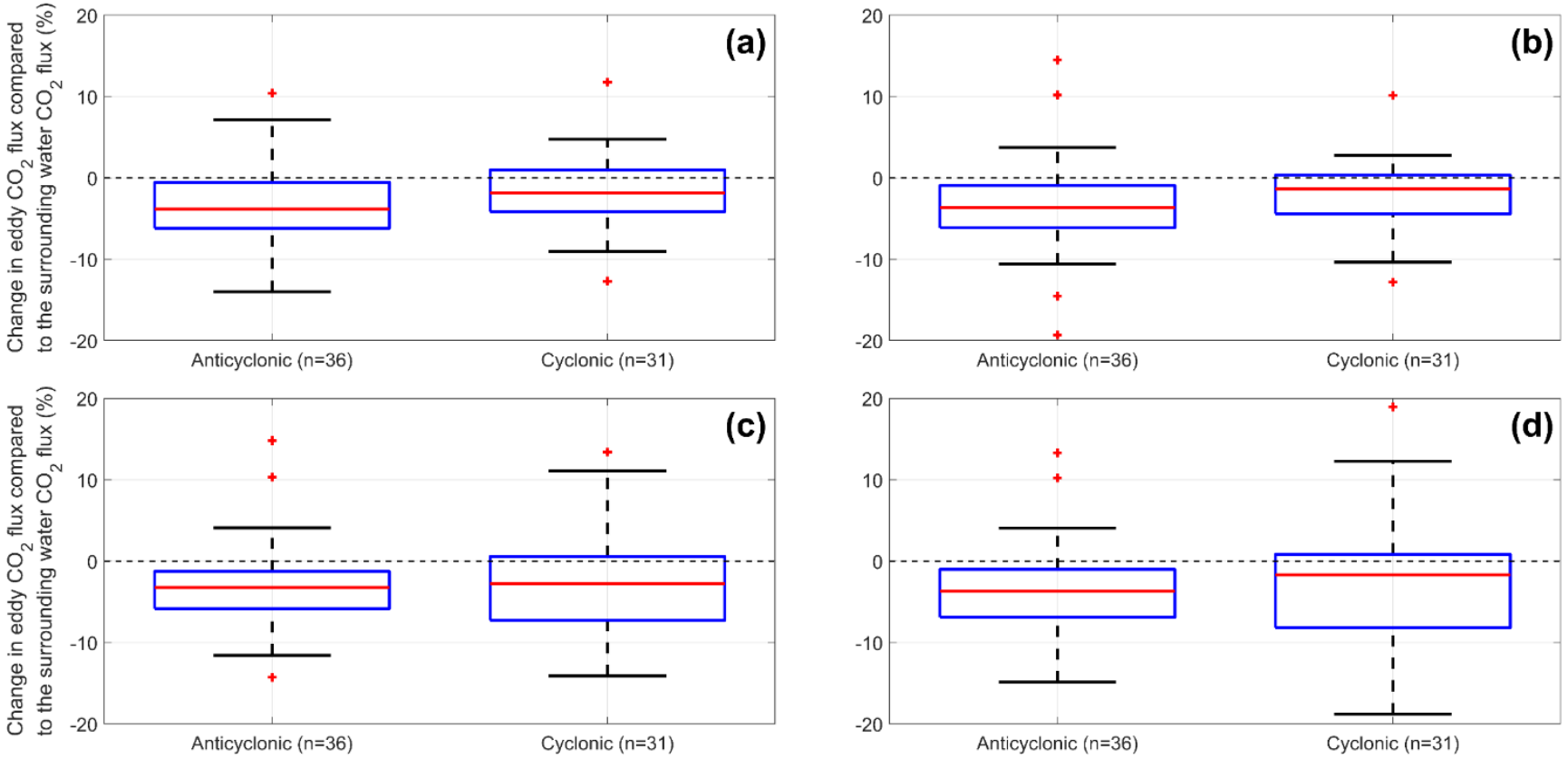

Figure S5: Box plots indicating the percent change in the cumulative net CO_2 flux at eddy dissipation with respect to the waters surrounding the eddy, using different radii to determine the surrounding water flux. (a) is 2 radii, (b) is 3 radii (as in Figure 2c), (c) is 4 radii and (d) is 5 radii. In each plot the red line indicates the median, blue box indicates the 25th and 75th percentile and whiskers show the minimum and maximum non-outlier values. Red crosses indicate outliers that are more than 1.5 times the interquartile range from the 25th and 75th percentiles. Negative percentages indicate a stronger flux, where positive percentages indicate a weaker flux.

References

Dickson, A. G. (1990). Standard potential of the Standard potential of the reaction - AgCl(s)+1/2H-2(g)=Ag(s)+HCl(aq) and the standard acidity constant of the ion HSO4- in synthetic sea-water from 273.15-K to 318.15-K. *The Journal of Chemical Thermodynamics*, *22*(2), 113–127. https://doi.org/10.1016/0021-9614(90)90074-Z

Ford, D. J., Tilstone, G. H., Shutler, J. D., & Kitidis, V. (2022). Derivation of seawater pCO_2 from net community production identifies the South Atlantic Ocean as a CO_2 source. *Biogeosciences*, *19*(1), 93–115. https://doi.org/10.5194/bg-19-93-2022

Goddijn-Murphy, L. M., Woolf, D. K., Land, P. E., Shutler, J. D., & Donlon, C. (2015). The OceanFlux Greenhouse Gases methodology for deriving a sea surface climatology of CO_2 fugacity in support of air-sea gas flux studies. *Ocean Science*, *11*(4), 519–541. https://doi.org/10.5194/os-11-519-2015

van Heuven, S., D. Pierrot, J. W. B. R., Lewis, E., & Wallace, D. W. R. (2011). *MATLAB Program Developed for CO_2 System Calculations*. Oak Ridge National Laboratory, Oak Ridge, TN: Carbon Dioxide Information Analysis Center. https://doi.org/10.3334/CDIAC/otg.CO2SYS_MATLAB_v1.1

Holding, T., Ashton, I. G., Shutler, J. D., Land, P. E., Nightingale, P. D., Rees, A. P., et al. (2019). The FluxEngine air–sea gas flux toolbox: simplified interface and extensions for in situ analyses and multiple sparingly soluble gases. *Ocean Science*, *15*(6), 1707–1728. https://doi.org/10.5194/os-15-1707-2019

Lewis, E., Wallace, D., & Allison, L. J. (1998). *Program developed for CO_2 system calculations*. Oak Ridge, TN. https://doi.org/10.2172/639712

Orr, J. C., Epitalon, J.-M., Dickson, A. G., & Gattuso, J.-P. (2018). Routine uncertainty propagation for the marine carbon dioxide system. *Marine Chemistry*, *207*, 84–107. https://doi.org/10.1016/j.marchem.2018.10.006

Orselli, I. B. M., Kerr, R., Azevedo, J. L. L. de, Galdino, F., Araujo, M., & Garcia, C. A. E. (2019). The sea-air CO_2 net fluxes in the South Atlantic Ocean and the role played by Agulhas eddies. *Progress in Oceanography*, *170*(2018), 40–52. https://doi.org/10.1016/j.pocean.2018.10.006

Reynolds, R. W., Rayner, N. A., Smith, T. M., Stokes, D. C., & Wang, W. (2002). An improved in situ and satellite SST analysis for climate. *Journal of Climate*, *15*(13), 1609–1625. https://doi.org/10.1175/1520-0442(2002)015<1609:AIISAS>2.0.CO;2

Sharp, J. D., Pierrot, D., Humphreys, M. P., Epitalon, J.-M., Orr, J. C., Lewis, E. R., & Wallace, D. W. R. (2021). CO2SYSv3 for MATLAB. https://doi.org/10.5281/ZENODO.4774718

Shutler, J. D., Land, P. E., Piolle, J. F., Woolf, D. K., Goddijn-Murphy, L., Paul, F., et al. (2016). FluxEngine: A flexible processing system for calculating atmosphere-ocean carbon dioxide gas fluxes and climatologies. *Journal of Atmospheric and Oceanic Technology*, *33*(4), 741–756. https://doi.org/10.1175/JTECH-D-14-00204.1

Waters, J., Millero, F. J., & Woosley, R. J. (2014). Corrigendum to “The free proton concentration scale for seawater pH”, [MARCHE: 149 (2013) 8–22]. *Marine Chemistry*, *165*, 66–67. https://doi.org/10.1016/j.marchem.2014.07.004

Woolf, D. K., Land, P. E., Shutler, J. D., Goddijn-Murphy, L. M., & Donlon, C. J. (2016). On the calculation of air-sea fluxes of CO_2 in the presence of temperature

and salinity gradients. *Journal of Geophysical Research: Oceans*, *121*(2), 1229–1248. https://doi.org/10.1002/2015JC011427